

Computed Aided Design and Simulation of a Dual Axis Sun Tracking Solar Panel Transmission

Saqer Ibrahim Al Ali & Jeremy (Zheng) Li

Department of Engineering

University of Bridgeport

126 Park Ave, Bridgeport, CT 06604, USA

Abstract

Sun tracking systems comprise of automated panels that follow solar emissions in order to achieve an optimal angle between radiations emitted from the sun and the solar panel. Once an optimal angle is identified, efficiency and the maximization of energy production can be achieved. Due to various locations of the sun, solar panels' efficiency and energy production are constrained. Therefore, in order to maximize the optimal angle, a dual axis tracking system designed to capture solar radiation will ensure that the solar panels maintain a perpendicular direction to the sun. The purpose of this thesis study is to design and simulate two slew drives that rotate the solar panel vertically and horizontally. In addition, material compression was conducted to select an optimal material with a minimum factor of safety of 2 which withstand the gust (wind) force in Connecticut. Our research determined that AISI 1050 Steel is the best material for the slew drives with a safety factor greater than 2 that can withstand the gusts during hot and cold weather conditions in Connecticut.

Keywords: SOLIDWORKS, ANSYS, slew drive, dual axis, safety factor, solar energy, wind load

1. Introduction

Solar energy generated by the sun is a major source of renewable electricity. It is useful in locations where electrical power supplied is inaccessible. This energy source is quickly gaining prominence due to the fluctuating petroleum fuel prices throughout global markets. Currently, the most popular reliable renewable energy around the world is solar energy. The solar systems are being continuously developed in these years, but few research works have been done in computational simulation on solar tracking system design and development (Li, 2013).

The solar trackers are made up of automated solar panels that orient themselves parallel to the solar radiation, and by doing so, they take full advantage of the optimal angle between the solar radiations and solar panels thereby improving efficiency and maximum energy production. The location of the sun fluctuates because of the continuous rotation of the planet earth. As a result, the optimal angle between the sun and solar panels must be maintained by free solar panels. Thus, the solar tracker is composed of movable panels that make use of specialized gears and motors to direct the tracker as signaled by an electronic controller about the direction of the solar radiations. In addition, the solar panel system should have the capability to store solar energy while withstanding gusts and heavy snow loads (Li, 2014).

The sun-tracking device tracks the sun movements by moving to positions that will offer optimum absorption without disruption. When the solar panels receive the solar radiations, the sensor placed on the solar panels will send a signal to the circuit board to tell the slew drive to move to a specific axis. For instance, when the sun rises, the sensor will be perpendicular with the incident rays absorbed on the solar panels. As the earth rotates, the position of the sun automatically shifts, and this will make the incident rays to change as well. This will make the light fall on the sensor placed on the either sides of the solar panels since the tracking circuit is designed in a way that when the light falls on the sensor on the right aspect of the panel, the tracker automatically moves to the left. Similarly, when the solar rays fall on the sensor on the left side, the tracker automatically rotates to the right side. At the same time when the sensor connected to the top surface of the solar panels, the electronic circuit will make the tracker shift downwards. This principle elucidates the working of the sun-tracker in line to the incident rays. Then, the absorbed rays are transformed into electric power by the photovoltaic cells found in the panels. Concisely, the automated solar tracker is responsible for the two rotational categories namely vertical as well as horizontal axis hence the dual axis solar tracker (Abdallah & Nijmeh, 2004).

The solar trackers give higher electrical power when compared with the stationary panels. However, the installation cost of the entire system is higher as compared to the stationary PV (Li, Tang, & Zhong, 2012). The central considerations that should be practical to the fixed panels are that they must be situated in a clear line of sight wide-open to the solar radiations. Similarly, the panels should be placed in an optimal position that faces the equator about the earth's latitude. In the same way, the PV panels do not entirely use the energy from the sun since Earth is always rotating in a tilted position. Therefore, the electrical output of the solar panels varies during the day even throughout the year. To address the problem of the optimizing the solar radiations, the use of solar tracking machines will evidently solve the problem of tracking the sun along the sky. The PV has shown about 30 percent efficiency while the sun tracking system has an efficiency of about 36 percent under normal conditions (Dolara et al., 2012).

Solar energy is used in distillation, where the process of desalination of salty water occurs in arid as well as coastal regions. The hot sun is utilized in transforming salty water into distilled water by solar distillation process. The process of solar distillation involves the transfer of solar radiation through transparent cover to a dark container that has salty water. As the radiation transmits to the covers, it is converted to heat energy by the black surface, which leads to the evaporation of water from the sodium chloride solution. The water vapors then undergo condensation to form distilled water. Finally, the purified water flows downwards where it is collected in sterile containers positioned at the bottommost part of the tank (Li, 2011).

Solar energy has the potential to reduce electricity bills of households since solar energy can be used to supplement other sources of energy. The amount of electricity that can be accumulated depends on the size and magnitude of the solar panel system as well as the household consumption of electricity. Also, the use of solar energy will ensure that more power is generated by a grid system for export to earn more foreign exchange (Mekhilef, Saidur, & Safari, 2011).

Solar tracking systems energy efficiency will drop significantly during hot climate zones more than in cold climate regions. There was an increase of 38% efficiency in solar irradiation in cold climate regions whereas there was only 8% increase in hot climate zones. Therefore, it is not economical to track the sun in hot or sunny regions due to overheating of crystalline silicon in solar panels, which effect their total performance while it is highly recommended to use them in cold and cloudy regions (Eldin, Abd-Elhady, & Kandil, 2016).

2. Design and Analysis:

2.1 Solar panel

The solar panel is a collection of solar cells that made of silicon material while the frame of the panel and other components are made of steel (Figure 2.0). The material of the panel was used because of; firstly, the mono-crystalline panel is long lasting and durable when compared to the polycrystalline panel. Secondly, the photovoltaic panels made of mono-crystalline cells are efficient regarding electrical power production. The panel can adapt the highest quantity of solar energy to electricity.

Likewise, the mono-crystalline have the capacity to offer a lesser level of the embedded amount of energy in each panel. The embodied energy is the total energy required to create a product and successfully supply it. With the mono-crystalline panel, the overall cost is lesser than that of a polycrystalline panel. Similarly, the panel of choice is environmentally friendly when compared to the thin solar product. The mono-crystalline panel does not contain the heavy metal cadmium, which has been found to accumulate in humans and animals and have significantly been linked to be one of the causes of cancer in both humans as well as animals (Gohlke, Hrynkow, & Portier, 2008). The other advantage of the mono-crystalline solar panel is that the loss of efficiency when the temperature rises to 50 degrees Celsius is lesser when compared with the polycrystalline cell. The cells as well have the ability to produce more electric power per meter square. Therefore, the mono-crystalline solar panel is used because they are cost effective, they are efficient apart from being reliable, and a bulk form of silicon is utilized in the prior technology (Nogueira, Bedin, Niedzialkoski, Souza, & Neves, 2015).

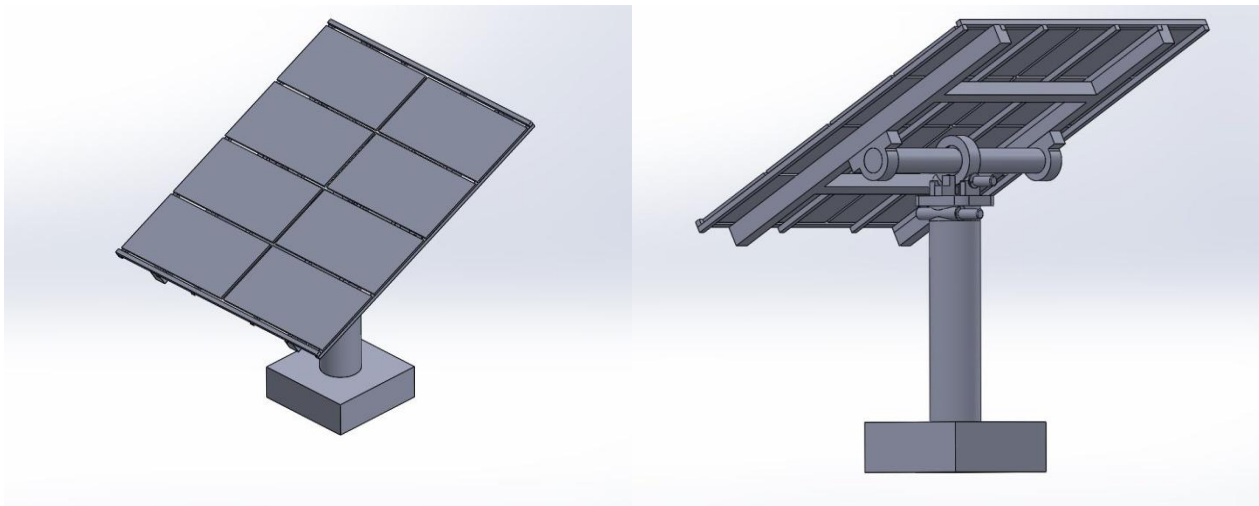


Figure 2.0: Dual Axis Sun Tracking Solar Panel Model

2.2 The Slewing Drive

The slewing drive was used in this thesis to produce a rotational torque, and it is mainly found in wind turbines, cranes and other machines that move during their normal operations (Fig 2.1). Furthermore, it was used as a moving mechanism for vertical and horizontal movements. The slewing drive was self-locking and irreversible to resist the wind and other forces that might interfere with the movement of the solar panels. It was made by combining gears, bearing and seals in a single unit. Additionally, the worm gear (Fig. 2.2) was used as a rotational movement by connecting the motor, horizontally; when the worm rotates, it also rotates the gear.

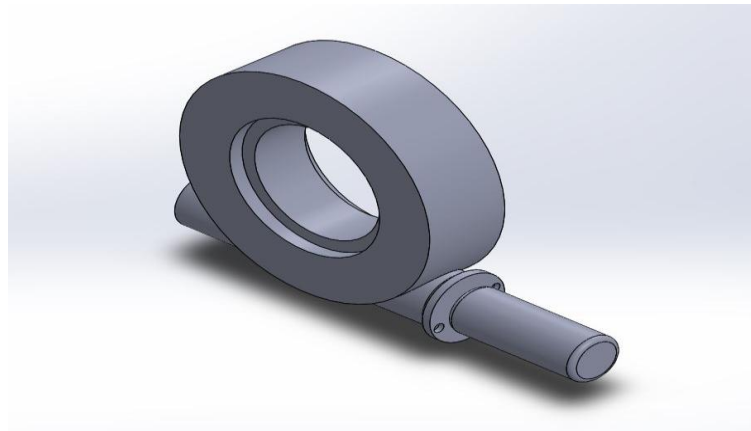


Figure 2.1: Slew Drive Model

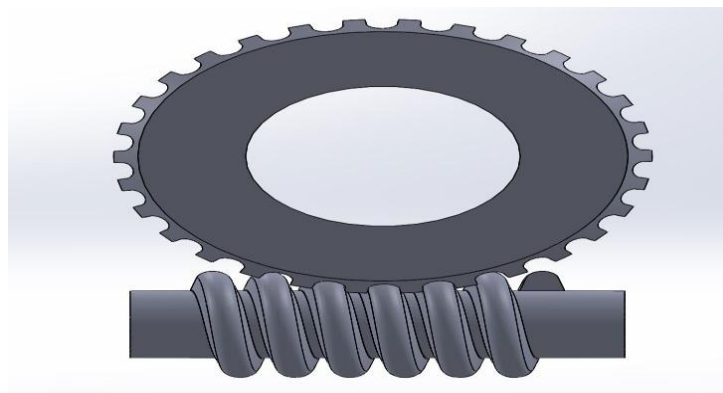


Figure 2.2: Worm Gear Model

2.3 Wind Load Analysis

Solar tracking systems are meant to work outside, with the potential loads coming from the atmospheric wind. The atmospheric pressures estimate the action of wind and its effect greatly depends on the wind parameters such as velocity, the turbulence characteristics, the dynamic factors, structural characteristics, and location. The design standards such as the ASCE 7-05 will provide procedures that will be used in the estimation of wind loads on the PV solar panels; the standard provides the models of wind action on the inclined surfaces of the PV platforms (ASCE 7-05, 2006). The wind force acting on the PV can be determined by the expression:

$$F_{wind} = q_z G C_f A_f (N) \quad (2-1) \text{(ASCE 7-05, 2006)}$$

where $\{q_z = \text{wind velocity pressure } (\frac{N}{m^2})\}$, G is gust effect factor C_f = the panel's force coefficient found in Table 2.0 and A_f = projected area of the panel normal to wind (m^2). The velocity pressure relation likewise is determined by this expression:

$$q_z = 0.613 k_z k_{zt} k_d V^2 I \left(\frac{N}{m^2}\right) \quad (2-2) \text{(ASCE 7-05, 2006)}$$

where $\{k_z = \text{velocity pressure exposure coefficients, which will be found in Table 2.1, } k_{zt} = \text{topographic factor, } k_d = \text{wind directionality factor which will be found in Table 2.2, } V = \text{wind velocity which in Connecticut is } 54 \frac{m}{s}$ (see Fig 2.9) and $I = \text{importance factor which will be found in Table 2.3. For the solar panel, the occupancy category should be I (Table 2.4)}\}$. The topographic factor relation will be determined by this expression:

$$k_{zt} = (1 + k_1 k_2 k_3)^2 \quad (2-3) \text{(ASCE 7-05, 2006)}$$

Since the solar panel is not located on the top of hills, the topographic factor will be equal to 1.

The gust effect factor relation will be determined by this expression:

$$G = 0.925 \left(\frac{1 + 1.7 g_Q I_z Q}{1 + 1.7 g_V I_z} \right) \quad (2-4) \text{(ASCE 7-05, 2006)}$$

$$I_z = c \left(\frac{10}{z} \right)^{\frac{1}{6}} \quad (2-5) \text{(ASCE 7-05, 2006)}$$

where $I_z = \text{the turbulence intensity at height } z$ where $z = \text{the equivalent height of the solar panel defined as } 0.6h$, but not less than z_{min} for the solar panel height h . z_{min} and c are listed for each exposure in Table 2.5; g_Q and g_V will be taken as 2.4. The background response Q is given by:

$$Q = \sqrt{\frac{1}{1 + 0.63 \left(\frac{B+h}{L_z} \right)^{0.63}}} \quad (2-6) \text{(ASCE 7-05, 2006)}$$

where $B = \text{horizontal dimension of the panel normal to the wind direction, } h = \text{height of the panel and } L_z = \text{the integral length scale of turbulence at the equivalent height given by:}$

$$L_z = \ell \left(\frac{z}{10} \right)^{\bar{e}} \quad (2-7) \text{(ASCE 7-05, 2006)}$$

where ℓ and \bar{e} are constants listed in Table 2.5.

After we find the wind force acting on the solar panel, we will use torque equation to find the force acting on the gear teeth determined by this expression:

$$F_{wind} L_{panel} = F_{gear} L_{gear} (N.m) \quad (2-8)$$

where $L_{panel} = \text{the horizontal or vertical length of the panel from the center, } F_{gear} = \text{the force acting on the gear and } L_{gear} = \text{the gear pitch radius.}$

After we find F_{gear} , we are going to multiply it by 2 to make sure that the gear is going to rotate the solar panel with negligible wind resistance and then we divide it by 3 for distributing the force on the three teeth.

2.4 ANSYS Design Modeling

2.4.1 Mesh

The size function of the mesh is adaptive, the relevance center is medium, the transition is fast, and the span angle center is medium. Since student edition has a limited number of elements and nodes, a finer mesh cannot be conducted. The number of nodes are 19854 and the number of elements are 10863.

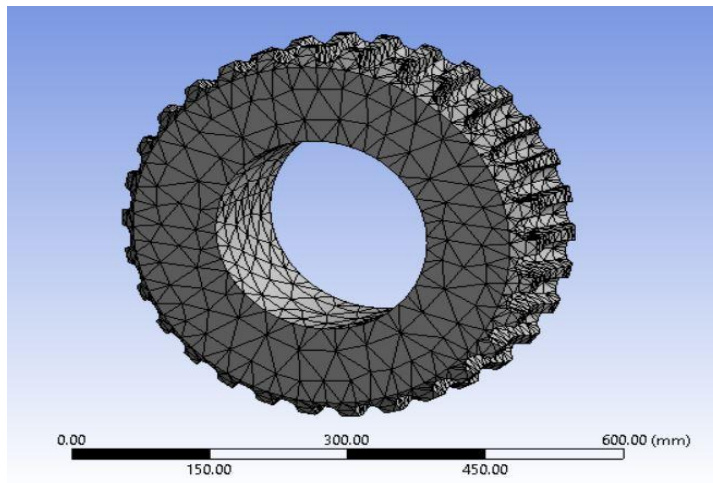


Figure 2.3: Mesh of the gear

2.4.2 Static Structural

The forces on the teeth are acting on the x component.

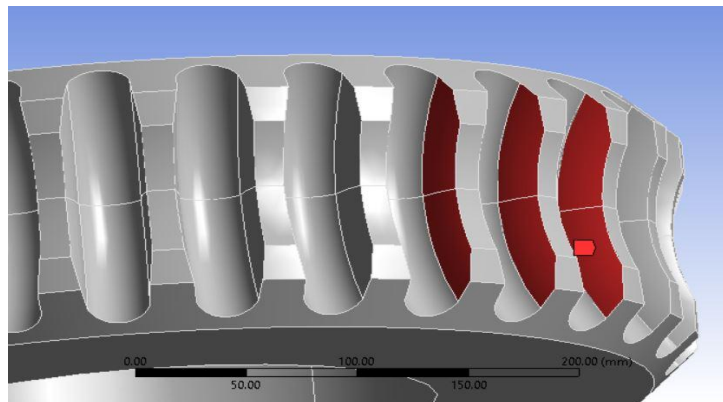


Figure 2.4: Force distributed on three teeth

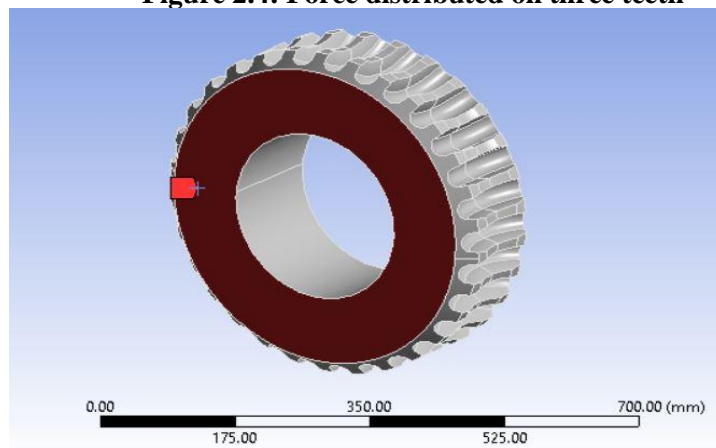


Figure 2.5: Weight acting on the surface of a horizontal gear

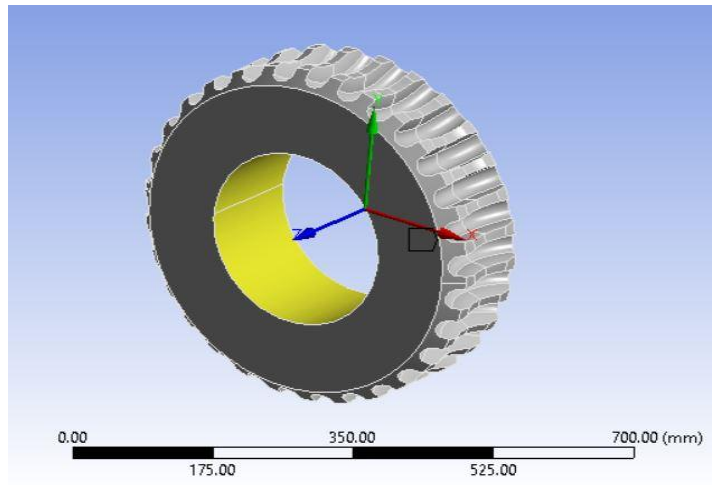


Figure 2.6: Displacement

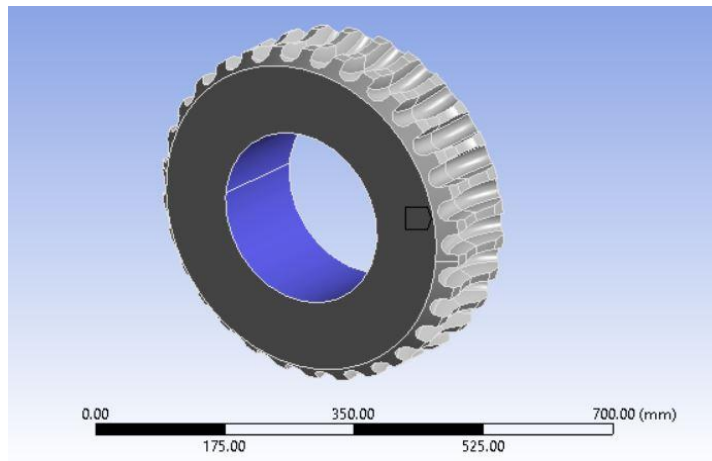


Figure 2.7: Frictionless Support

The thermal condition is emphasized in the analysis due to the behavior of the material during hot and cold temperature as it expand and contrast, respectively. Because the panel will be used in Connecticut, the temperatures will be 40 degrees Celsius and -5 degrees Celsius.

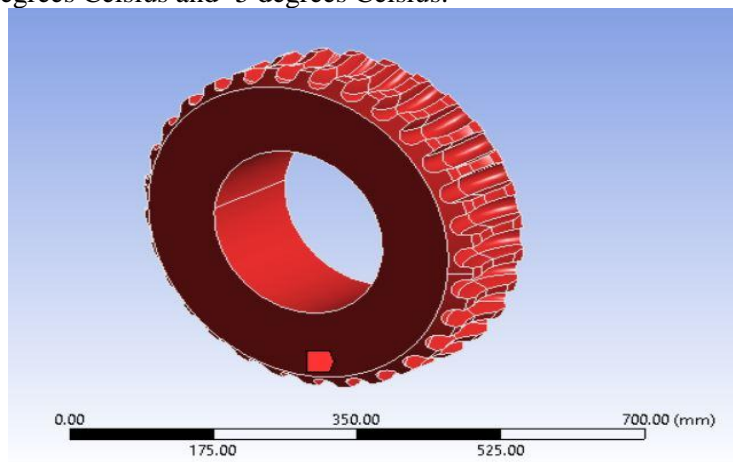


Figure 2.8: Thermal Condition

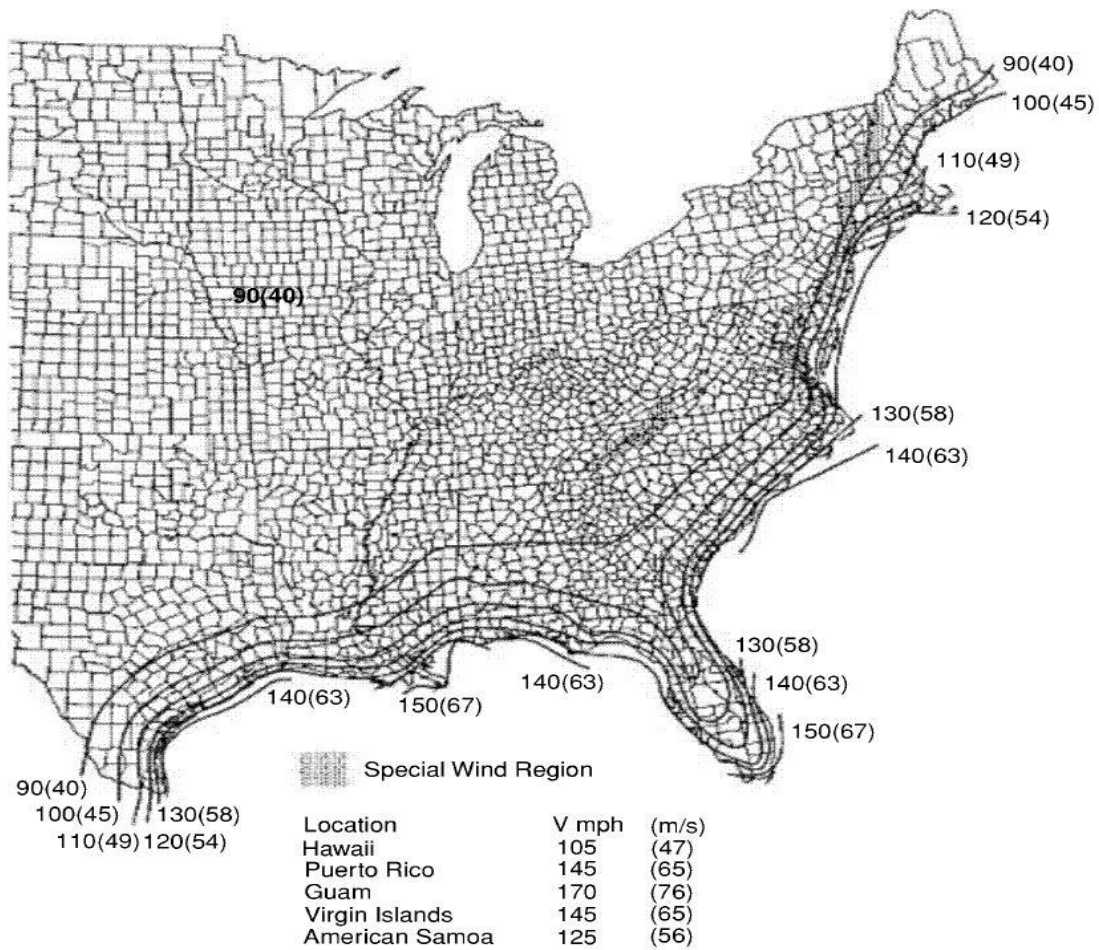


Figure 2.9: Wind Speed in the United States

Note: Reprinted from Design Loads for Buildings and Other Structures, ASCE. Copyright 2006 by ASCE.

Cross-Section	Type of Surface	h/D		
		1	7	25
Square (wind normal to face)	All	1.3	1.4	2.0
Square (wind along diagonal)	All	1.0	1.1	1.5
Hexagonal or octagonal	All	1.0	1.2	1.4
Round ($D\sqrt{q_z} > 2.5$) ($D\sqrt{q_z} > 5.3$, D in m, q_z in N/m^2)	Moderately smooth	0.5	0.6	0.7
	Rough ($D'/D = 0.02$)	0.7	0.8	0.9
	Very rough ($D'/D = 0.08$)	0.8	1.0	0.2
Round ($D\sqrt{q_z} \leq 2.5$) ($D\sqrt{q_z} \leq 5.3$, D in m, q_z in N/m^2)	All	0.7	0.8	1.2

Notes:

- The design wind force shall be calculated based on the area of the structure projected on a plane normal to the wind direction. The force shall be assumed to act parallel to the wind direction.
- Linear interpolation is permitted for h/D values other than shown.
- Notation:
 - D : diameter of circular cross-section and least horizontal dimension of square, hexagonal or octagonal cross-sections at elevation under consideration, in feet (meters);
 - D' : depth of protruding elements such as ribs and spoilers, in feet (meters); and
 - h : height of structure, in feet (meters); and
 - q_z : velocity pressure evaluated at height z above ground, in pounds per square foot (N/m^2).

Table 2.0: Force Coefficient

Note: Reprinted from Design Loads for Buildings and Other Structures, ASCE. Copyright 2006 by ASCE.

Height above ground level, z		Exposure (Note 1)			
		B		C	D
ft	(m)	Case 1	Case 2	Cases 1 & 2	Cases 1 & 2
0-15	(0-4.6)	0.70	0.57	0.85	1.03
20	(6.1)	0.70	0.62	0.90	1.08
25	(7.6)	0.70	0.66	0.94	1.12
30	(9.1)	0.70	0.70	0.98	1.16
40	(12.2)	0.76	0.76	1.04	1.22
50	(15.2)	0.81	0.81	1.09	1.27
60	(18)	0.85	0.85	1.13	1.31
70	(21.3)	0.89	0.89	1.17	1.34
80	(24.4)	0.93	0.93	1.21	1.38
90	(27.4)	0.96	0.96	1.24	1.40
100	(30.5)	0.99	0.99	1.26	1.43
120	(36.6)	1.04	1.04	1.31	1.48
140	(42.7)	1.09	1.09	1.36	1.52
160	(48.8)	1.13	1.13	1.39	1.55
180	(54.9)	1.17	1.17	1.43	1.58
200	(61.0)	1.20	1.20	1.46	1.61
250	(76.2)	1.28	1.28	1.53	1.68
300	(91.4)	1.35	1.35	1.59	1.73
350	(106.7)	1.41	1.41	1.64	1.78
400	(121.9)	1.47	1.47	1.69	1.82
450	(137.2)	1.52	1.52	1.73	1.86
500	(152.4)	1.56	1.56	1.77	1.89

Notes:

- Case 1:**
 - All components and cladding.
 - Main wind force resisting system in low-rise buildings designed using Figure 6-10.
- Case 2:**
 - All main wind force resisting systems in buildings except those in low-rise buildings designed using Figure 6-10.
 - All main wind force resisting systems in other structures.
- The velocity pressure exposure coefficient K_z may be determined from the following formula:

For $15 \text{ ft.} \leq z \leq z_g$	For $z < 15 \text{ ft.}$
$K_z = 2.01 (z/z_g)^{2/\alpha}$	$K_z = 2.01 (15/z_g)^{2/\alpha}$

Note: z shall not be taken less than 30 feet for Case 1 in exposure B.

Table 2.1: Velocity Pressure Exposure Coefficients

Note: Reprinted from Design Loads for Buildings and Other Structures, ASCE. Copyright 2006 by ASCE.

Structure Type	Directionality Factor K_d^*
Buildings	
Main Wind Force Resisting System	0.85
Components and Cladding	0.85
Arched Roofs	0.85
Chimneys, Tanks, and Similar Structures	
Square	
Hexagonal	0.90
Round	0.95
	0.95
Solid Signs	0.85
Open Signs and Lattice Framework	0.85
Trussed Towers	
Triangular, square, rectangular	0.85
All other cross sections	0.95

Table 2.2: Wind Directionality Factor

Note: Reprinted from Design Loads for Buildings and Other Structures, ASCE. Copyright 2006 by ASCE.

Category	Non-Hurricane Prone Regions and Hurricane Prone Regions with V = 85-100 mph and Alaska	Hurricane Prone Regions with V > 100 mph
I	0.87	0.77
II	1.00	1.00
III	1.15	1.15
IV	1.15	1.15

Table 2.3: Importance Factor

Note: Reprinted from Design Loads for Buildings and Other Structures, ASCE. Copyright 2006 by ASCE.

Nature of Occupancy	Occupancy Category
Buildings and other structures that represent a low hazard to human life in the event of failure, including, but not limited to: <ul style="list-style-type: none"> • Agricultural facilities • Certain temporary facilities • Minor storage facilities 	I
All buildings and other structures except those listed in Occupancy Categories I, III, and IV	II
Buildings and other structures that represent a substantial hazard to human life in the event of failure, including, but not limited to: <ul style="list-style-type: none"> • Buildings and other structures where more than 300 people congregate in one area • Buildings and other structures with daycare facilities with a capacity greater than 150 • Buildings and other structures with elementary school or secondary school facilities with a capacity greater than 250 • Buildings and other structures with a capacity greater than 500 for colleges or adult education facilities • Health care facilities with a capacity of 50 or more resident patients, but not having surgery or emergency treatment facilities • Jails and detention facilities Buildings and other structures, not included in Occupancy Category IV, with potential to cause a substantial economic impact and/or mass disruption of day-to-day civilian life in the event of failure, including, but not limited to: <ul style="list-style-type: none"> • Power generating stations^d • Water treatment facilities • Sewage treatment facilities • Telecommunication centers Buildings and other structures not included in Occupancy Category IV (including, but not limited to, facilities that manufacture, process, handle, store, use, or dispose of such substances as hazardous fuels, hazardous chemicals, hazardous waste, or explosives) containing sufficient quantities of toxic or explosive substances to be dangerous to the public if released. Buildings and other structures containing toxic or explosive substances shall be eligible for classification as Occupancy Category II structures if it can be demonstrated to the satisfaction of the authority having jurisdiction by a hazard assessment as described in Section 1.5.2 that a release of the toxic or explosive substances does not pose a threat to the public.	III
Buildings and other structures designated as essential facilities, including, but not limited to: <ul style="list-style-type: none"> • Hospitals and other health care facilities having surgery or emergency treatment facilities • Fire, rescue, ambulance, and police stations and emergency vehicle garages • Designated earthquake, hurricane, or other emergency shelters • Designated emergency preparedness, communication, and operation centers and other facilities required for emergency response • Power generating stations and other public utility facilities required in an emergency • Ancillary structures (including, but not limited to, communication towers, fuel storage tanks, cooling towers, electrical substation structures, fire water storage tanks or other structures housing or supporting water, or other fire-suppression material or equipment) required for operation of Occupancy Category IV structures during an emergency • Aviation control towers, air traffic control centers, and emergency aircraft hangars • Water storage facilities and pump structures required to maintain water pressure for fire suppression • Buildings and other structures having critical national defense functions Buildings and other structures (including, but not limited to, facilities that manufacture, process, handle, store, use, or dispose of such substances as hazardous fuels, hazardous chemicals, or hazardous waste) containing highly toxic substances where the quantity of the material exceeds a threshold quantity established by the authority having jurisdiction. Buildings and other structures containing highly toxic substances shall be eligible for classification as Occupancy Category II structures if it can be demonstrated to the satisfaction of the authority having jurisdiction by a hazard assessment as described in Section 1.5.2 that a release of the highly toxic substances does not pose a threat to the public. This reduced classification shall not be permitted if the buildings or other structures also function as essential facilities.	IV

^dCogeneration power plants that do not supply power on the national grid shall be designated Occupancy Category II.

Table 2.4: Occupancy Category

Note: Reprinted from Design Loads for Buildings and Other Structures, ASCE. Copyright 2006 by ASCE.

Exposure	α	z_g (m)	\hat{a}	\hat{b}	$\bar{\alpha}$	\bar{b}	c	ℓ (m)	$\bar{\epsilon}$	z_{min} (m)*
B	7.0	365.76	1/7	0.84	1/4.0	0.45	0.30	97.54	1/3.0	9.14
C	9.5	274.32	1/9.5	1.00	1/6.5	0.65	0.20	152.4	1/5.0	4.57
D	11.5	213.36	1/11.5	1.07	1/9.0	0.80	0.15	198.12	1/8.0	2.13

* z_{min} = minimum height used to ensure that the equivalent height \bar{z} is greater of $0.6h$ or z_{min} .
 For buildings with $h \leq z_{min}$, \bar{z} shall be taken as z_{min} .

Table 2.5: Exposure Constants

Note: Reprinted from Design Loads for Buildings and Other Structures, ASCE. Copyright 2006 by ASCE.

3.Results and Discussion:

The force distributed on the three teeth for the horizontal worm gear was found to be 96486.2 N while the vertical worm gear was found to be 78626.97 N. The results obtained from the ANSYS simulation over the worm gear will be presented. The simulation has been tested in different temperatures at 22° C, 40° C and -5° C. Comparison between results obtained from the ANSYS simulation was made to validate the optimal material in these conditions. AISI 1050 Steel is used in this analysis. It is important to note that vertical and horizontal worm gears results show insignificant difference. Therefore, this result showing only the horizontal worm gear as the base model.

3.1 At 22° C Temperature

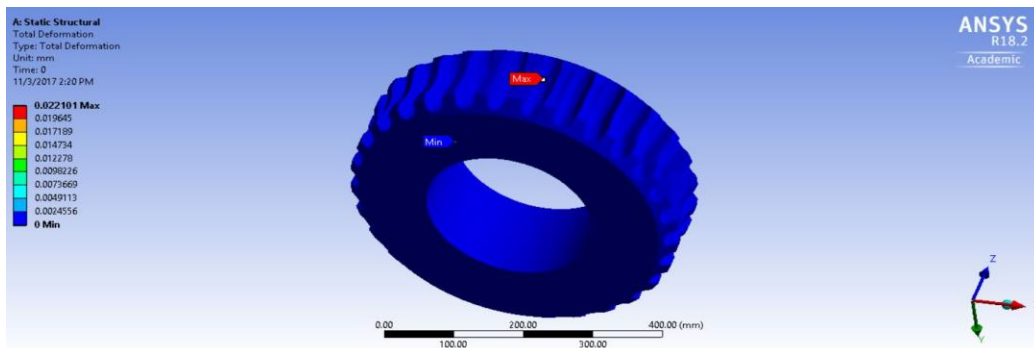
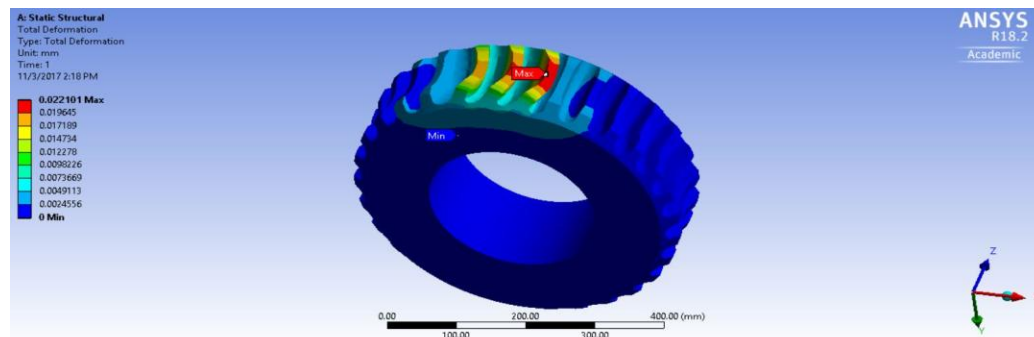


Figure 3.0: Total Deformation (before)

Figure 3.1: Total Deformation



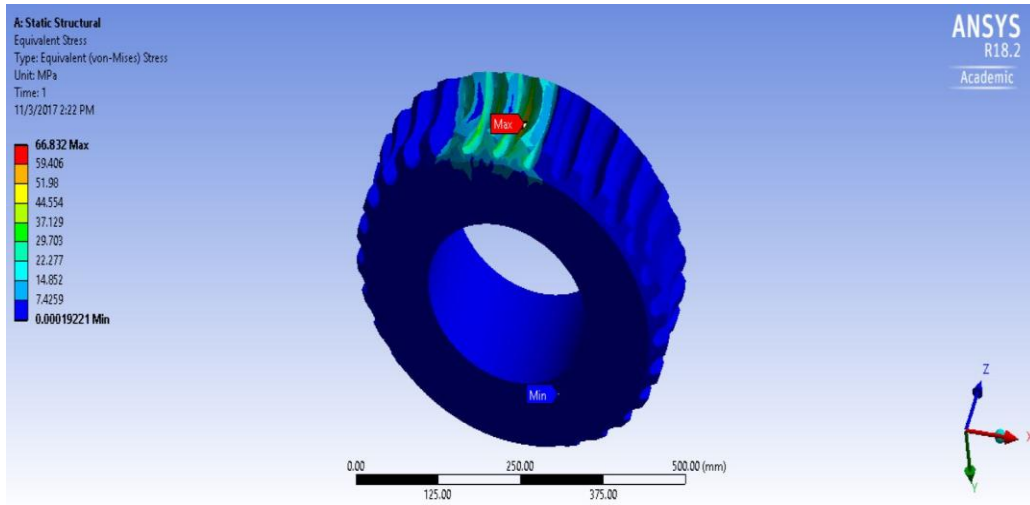


Figure 3.2: Equivalent Stress

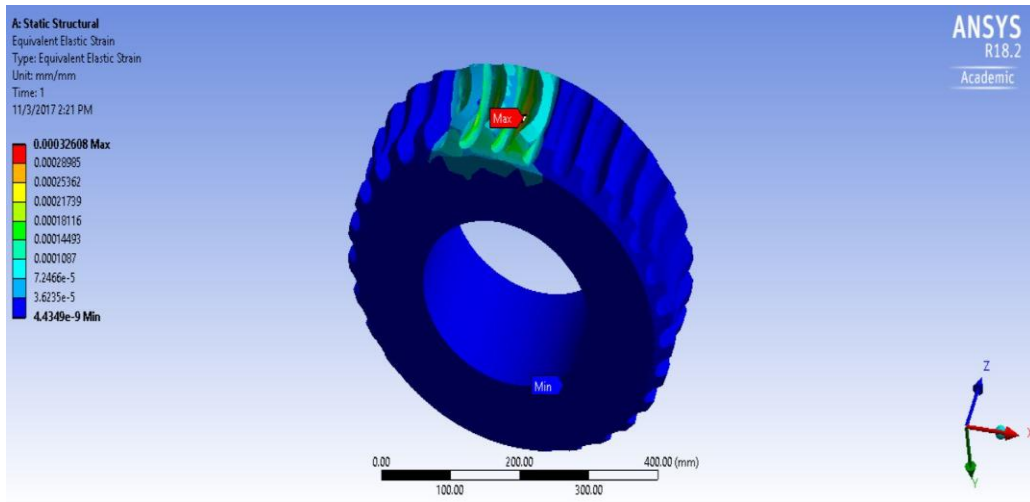


Figure 3.3: Equivalent Elastic Strain

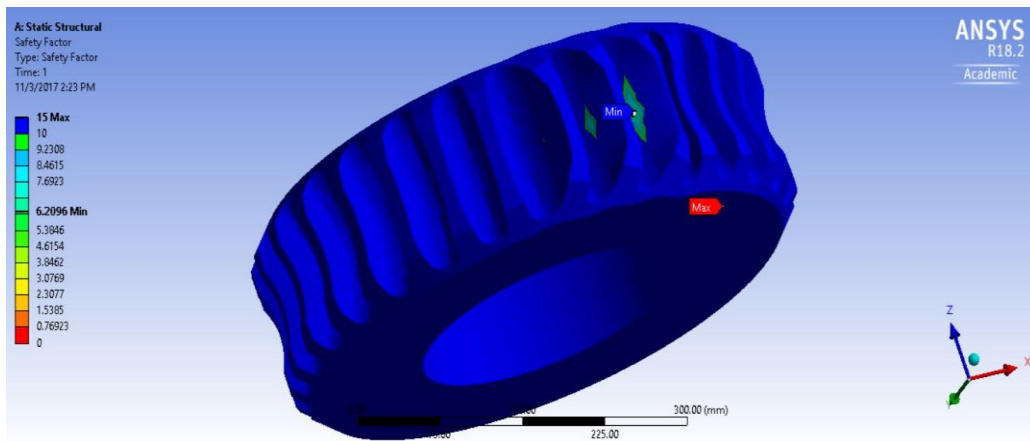


Figure 3.4: Factor of Safety

3.2 At 40° C Temperature

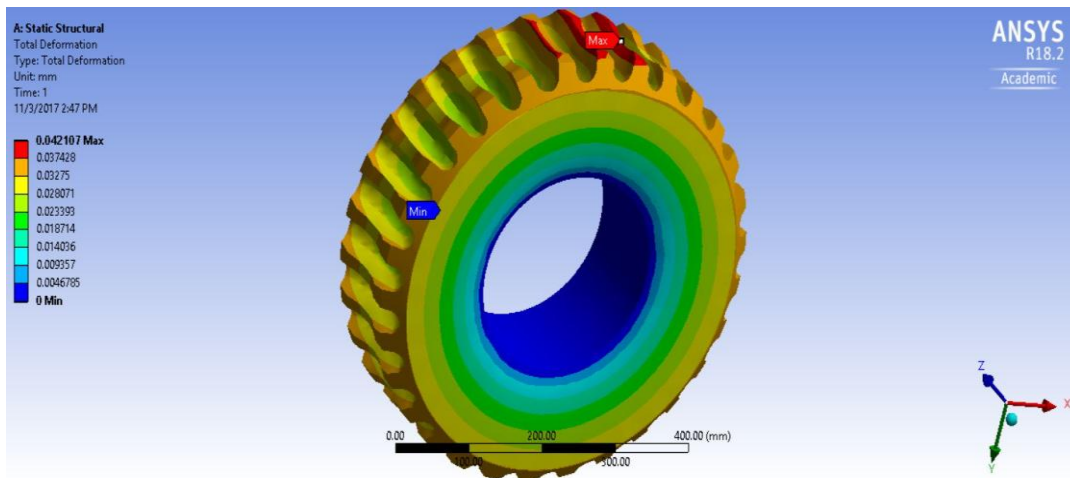


Figure 3.5: Total Deformation

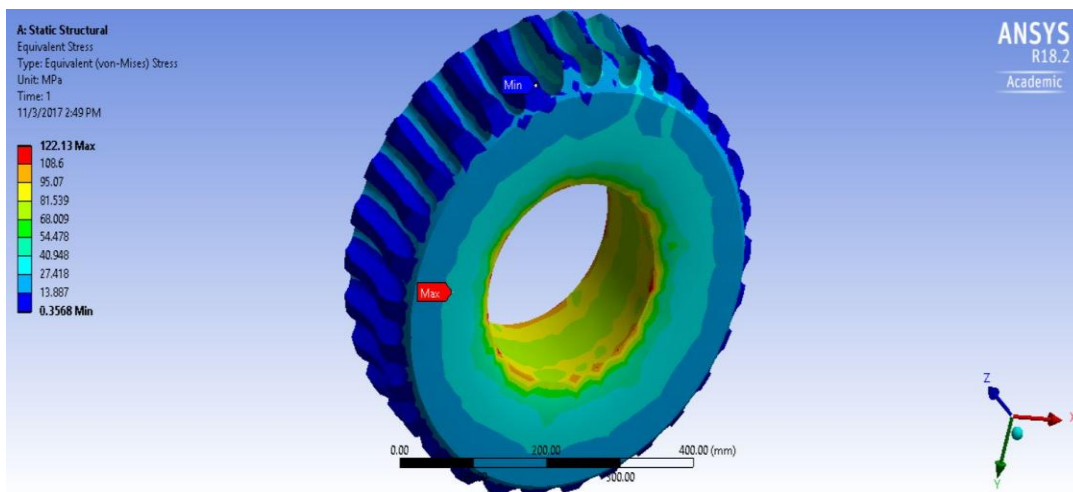


Figure 3.6: Equivalent Stress

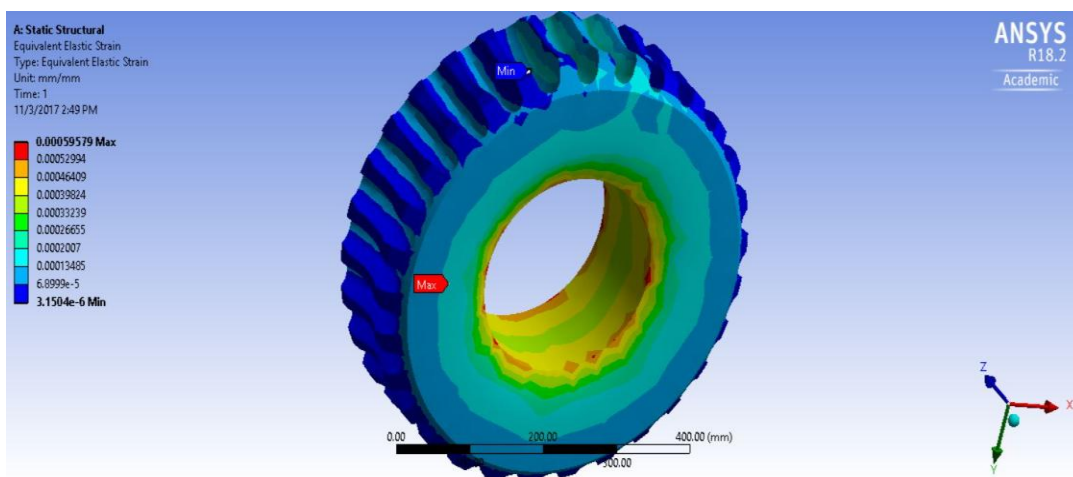


Figure 3.7: Equivalent Elastic Strain

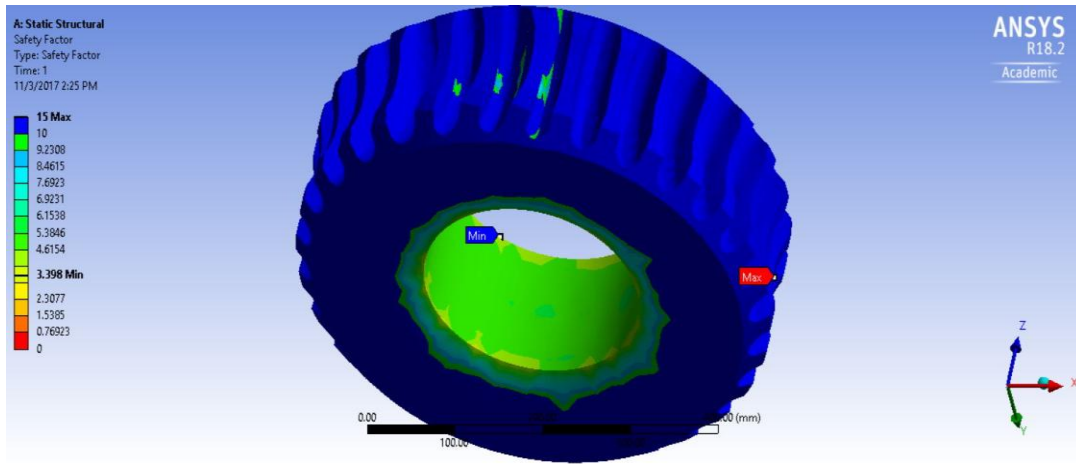


Figure 3.8: Factor of Safety

3.3 At -5° C Temperature

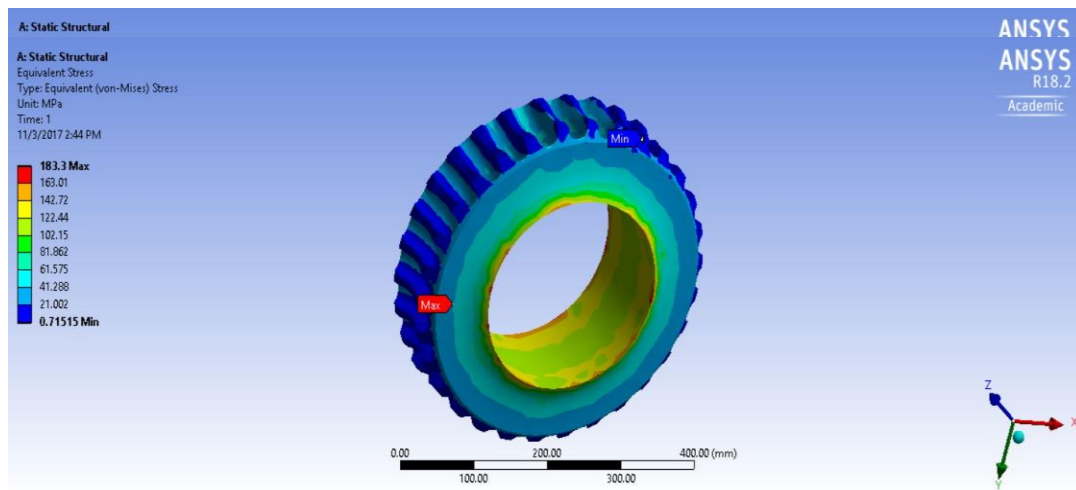


Figure 3.9: Total Deformation

Figure 3.10: Equivalent Stress

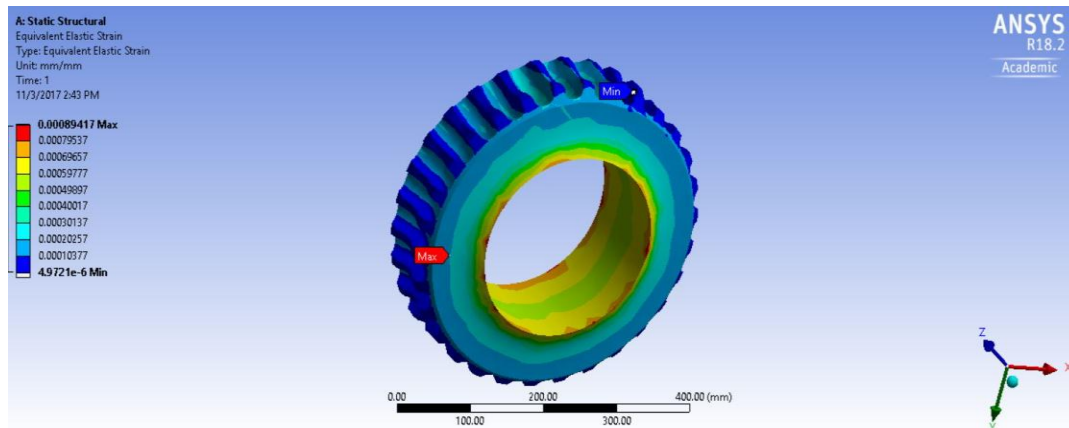


Figure 3.11: Equivalent Elastic Strain

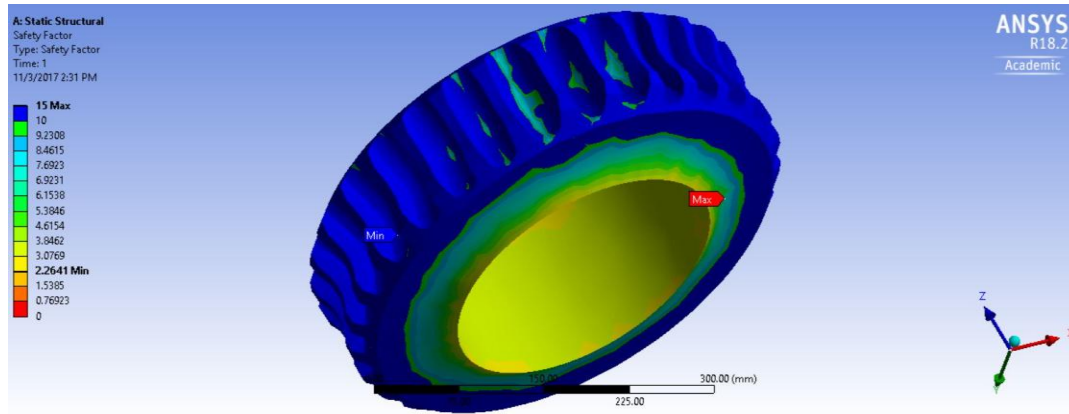


Figure 3.12: Factor of Safety

3.4 Material Selection

After the analysis have been conducted, several materials have been tested to meet the optimal requirement for this design. Matweb.com have been used as a reference for the material properties (Matweb, 2017). In addition, alibaba.com have been used for the average cost of materials per kg (Alibaba, 2017). Table 3.0 will discuss the comparison between materials:

Material	Thermal Condition (C)	Total Deformation (mm)	Equivalent Stress (MPa)	Equivalent Elastic Strain (mm/mm)	Safety Factor	Cost/kg (\$)
302 Stainless Steel (Annealed Bar)	22	0.023	67.49	0.00035	8.67	~1.65
	40	0.056	165.78	0.00086	3.53	
	-5	0.079	248.95	0.00129	2.35	
AISI 302B Stainless Steel (Annealed Bar)	22	0.023	67.49	0.00035	4.07	~1.65
	40	0.053	157.75	0.00081	1.74	
	-5	0.075	236.91	0.00125	1.16	
AISI 1050 Steel (Rolled)	22	0.022	66.83	0.00032	6.21	~0.66
	40	0.042	122.13	0.00060	3.40	
	-5	0.057	183.3	0.00089	2.26	
AISI 1030 Steel (Rolled)	22	0.022	66.83	0.00032	5.16	~0.55
	40	0.042	122.73	0.00060	2.8	
	-5	0.056	184.19	0.00089	1.87	
AISI 1020 Steel (Rolled)	22	0.024	66.83	0.00036	4.94	~0.55
	40	0.044	110.81	0.00060	2.98	
	-5	0.057	166.31	0.00089	1.98	
Titanium Alloy (Rolled)	22	0.047	65.79	0.00069	14.14	~15
	40	0.058	65.90	0.00069	14.11	
	-5	0.064	73.37	0.00076	12.68	

Table 3.0: Materials Behavior

Conclusion

AISI 1050 Steel is showed in the results as the best candidate for selecting the material for the slew drives which have a safety factor greater than 2 during hot and cold temperatures, which will also survive the gust of wind in the state of Connecticut. Other materials have not been selected because they are costlier, or the safety factor is below 2. In addition, the vertical and horizontal slew drives did not show significant differences when selecting the material.

References

- Abdallah, S., & Nijmeh, S. (2004). Two axes sun tracking system with PLC control. *Energy conversion and management*, 45(11), 1931-1939.
- Alibaba. (2017). Global Trade Starts Here. Retrieved from <http://www.alibaba.com>
- ASCE 7-05. (2006). Chapter 6 Wind Loads. In ASCE 7-05, *Design Loads for Buildings and Other Structures* (pp.21-80). American Society of Civil Engineers.
- Dolara, A., Grimaccia, F., Leva, S., Mussetta, M., Faranda, R., &Gualdoni, M. (2012). Performance analysis of a single-axis tracking PV system. *IEEE Journal of Photovoltaics*, 2(4), 524-531.
- Eldin, S. S., Abd-Elhady, M., &Kandil, H. (2016). Feasibility of solar tracking systems for PV panels in hot and cold regions. *Renewable Energy*, 85, 228-233.
- Gohlke, J. M., Hrynkow, S. H., &Portier, C. J. (2008). Health, Economy, and Environment: Sustainable Energy Choices for a Nation. *Environmental Health Perspectives*, 116(6).
- Li, G. H., Tang, R. S., &Zhong, H. (2012). Optical Performance of Horizontal Single-Axis Tracked Solar Panels. *Advanced Materials Research*, 424-425, 805-810.
- Li, J. (2011). Computer-Aided Design, Modeling and Simulation of a New Solar Still Design. *Modelling and Simulation in Engineering*, 2011, 1-5.
- Li, J. Z. (2013). Computer Aided Modeling and Prototyping of a New Industrial Solar Tracking System. *Journal on Future Engineering and Technology*, 8(2), 33-37.
- Li, J. Z. (2014). Computer Aided Design and Development of a New Solar Panel Tracking System. *Journal of Mechatronics*, 2(1), 17-21.
- Matweb. (2017). Material Property Data. Retrieved from <http://www.matweb.com>
- Mekhilef, S., Saidur, R., & Safari, A. (2011). A review on solar energy use in industries. *Renewable and Sustainable Energy Reviews*, 15(4), 1777-1790.
- Nogueira, C. E., Bedin, J., Niedzialkoski, R. K., Souza, S. N., &Neves, J. C. (2015). Performance of monocrystalline and polycrystalline solar panels in a water pumping system in Brazil. *Renewable and Sustainable Energy Reviews*, 51, 1610-1616.